

Modelling of the Exhaust Gas Temperature for Diesel Engines

Master's thesis
performed in **Vehicular Systems**
Performed for **Scania CV AB**
by
Pål Skogtjärn

Reg nr: LiTH-ISY-EX-3378-2002

13th December 2002

Modelling of the Exhaust Gas Temperature for Diesel Engines

Master's thesis

performed in **Vehicular Systems,**
Dept. of Electrical Engineering
at Linköpings universitet

Performed for **Scania CV AB**
by **Pål Skogtjärn**

Reg nr: LiTH-ISY-EX-3378-2002

Supervisors: **David Elfvik, MSc**
Scania CV AB
Magnus Petterson, PhD
Scania CV AB
Jonas Biteus, MSc
As the engine normally runs with α chosen by S6 this is not a major problem. Linköpings universitet

Examiner: **Assistant professor Lars Eriksson**
Linköpings universitet

Södertälje, 13th December 2002



Avdelning, Institution
Division, Department

Vehicular Systems,
Dept. of Electrical Engineering
581 83 Linköping

Datum
Date

13th December 2002

Språk Language	<input type="checkbox"/> Svenska/Swedish <input checked="" type="checkbox"/> Engelska/English <input type="checkbox"/> _____
--------------------------	--

Rapporttyp Report category	<input type="checkbox"/> Licentiatavhandling <input checked="" type="checkbox"/> Examensarbete <input type="checkbox"/> C-uppsats <input type="checkbox"/> D-uppsats <input type="checkbox"/> Övrig rapport <input type="checkbox"/> _____
--------------------------------------	---

ISBN —	ISRN LITH-ISY-EX-3378-2002
Serietitel och serienummer ISSN Title of series, numbering	—

URL för elektronisk version http://www.vehicular.isy.liu.se http://www.ep.liu.se/exjobb/isy/2002/3378/
--

Titel Modellering av avgastemperaturen hos dieselmotorer	
Title Modelling of the Exhaust Gas Temperature for Diesel Engines	
Författare Pål Skogtjärn	
Author	

Sammanfattning
Abstract
Models for the exhaust gas temperature are developed and validated for a turbo charged diesel engine. The area of use for the models are on-board diagnostics or model-based control. Data, for model building and validation, comes from measurements on a Scania turbo charged diesel engine equipped with variable geometry turbine and exhaust gas recirculation. Different models are validated and an extension of the ideal Seliger cycle is suggested as the model of choice.
With access to fuel and gas mass flows, inlet temperature and inlet and outlet pressures, the Seliger cycle model estimates the exhaust gas temperature.
Static validations are made with exhaust gas temperatures between 550 K and 950 K, at constant engine speed. Under these conditions the Seliger cycle model, with parameters fitted to engine data, show a maximum relative error of 2%. Without any parameter fitting to engine data, the maximum relative error is 5%.

Nyckelord
Keywords On-board diagnostics; Ideal cycle; VGT

Abstract

Models for the exhaust gas temperature are developed and validated for a turbo charged diesel engine. The area of use for the models are on-board diagnostics or model-based control. Data, for model building and validation, comes from measurements on a Scania turbo charged diesel engine equipped with variable geometry turbine and exhaust gas recirculation. Different models are validated and an extension of the ideal Seliger cycle is suggested as the model of choice.

With access to fuel and gas mass flows, inlet temperature and inlet and outlet pressures, the Seliger cycle model estimates the exhaust gas temperature.

Static validations are made with exhaust gas temperatures between 550 K and 950 K, at constant engine speed. Under these conditions the Seliger cycle model, with parameters fitted to engine data, show a maximum relative error of 2%. Without any parameter fitting to engine data, the maximum relative error is 5%.

Keywords: On-board diagnostics; Ideal cycle; VGT

Preface

This master's thesis has been performed for Scania at the division of Software and Diagnostics (NMCS) during summer/fall 2002.

Thesis outline

The outline of this thesis is described in the paragraphs below

Chapter 1, Introduction: Background and objectives of this thesis.

Chapter 2, Measurements: A brief presentation of the test engine and where different variables are measured.

Chapter 3, Modelling: Presentation of three different models and how to use these models during transients. The reader not familiar with ideal cycle calculations should look in Appendix A for derivation of the formulas in Section 3.2.

Chapter 4, Validation: Static and dynamic validations of the models in Chapter 3.

Chapter 5, Conclusions and Future Work: Discussion about the results presented in this thesis, and future work that can be done to improve the models.

Acknowledgments

First a thank you to my supervisors David Elfvik, Magnus Pettersson and Jonas Biteus for their help and support. I would also like to thank Lars Eriksson and Mattias Nyberg for taking their time helping me. At last i would like to thank all people at NMCS for making my time at Scania as good as it has been.

Pål Skogtjärn
Södertälje, November 2002

Contents

Abstract	v
Preface and Acknowledgment	vi
1 Introduction	1
2 Measurements	3
3 Modelling	5
3.1 Energy Balance Model	5
3.2 Ideal Cycle Models	6
3.2.1 Otto Cycle	6
3.2.2 Seliger Cycle	7
3.2.3 Summary	8
3.3 Dynamic Modelling	8
4 Validation	9
4.1 Energy Balance Model Validation	10
4.2 Ideal Cycle Model Validation	11
4.2.1 Otto Cycle	11
4.2.2 Seliger Cycle	11
4.2.3 Validation Observations for the Ideal Cycles . . .	13
4.3 Dynamic Validation	14
4.4 Summary	17
5 Conclusions and Future Work	19
5.1 Conclusions	19
5.2 Future Work	20
References	21
Notation	23

A Ideal Cycle Calculations	25
A.1 Otto Cycle	25
A.2 Seliger Cycle	28

Chapter 1

Introduction

Background

To reduce emissions from heavy duty trucks, legislative restrictions on emissions are getting more and more strict. Trying to meet these restrictions the manufacturers are using more complex engine systems to reduce emissions while maintaining performance and low fuel consumption. An approach to control these systems is to use model-based control and therefore models, e.g. equations or maps, of the different systems are required.

From 2005 all trucks sold in the EU must be equipped with an on-board diagnostics (OBD) system. The aim of this system is to make sure emission restrictions are kept, even when the truck is on duty. The OBD system should indicate increased emissions and isolate faulty components so that they can be replaced easily. Model-based diagnosis can be used for this and once again, good models for subsystems are needed. The output of a model can be compared with corresponding measured variable, and if they deviate from each other too much a fault has occurred (compare with residuals and thresholds [11]).

Models for different systems are useful in different ways and in addition to the ones indicated above, models can replace sensors and thereby lower the cost of the product.

Much work has been done in the field of creating mean value models for an entire engine [3, 9]. These models are normally fairly simple for each subsystem and often engine data is used to build these models.

Objectives

The objective of this master's thesis is to create a model of the exhaust gas temperature (T_{em}) on a turbo charged diesel engine with variable

geometry turbine (VGT [5]) and exhaust gas recirculation (EGR [2]) systems.

The model should preferably be physical (no fit to data), accurate and easily calculated as the computing power in the vehicle is limited. As T_{em} is determined by the combustion, and the combustion is very complex, all three desired characteristics for the model can not be fulfilled. The different models presented in this thesis are somewhere between physical, accurate and easily calculated.

Methods

Data from a Scania (12 liter, 6 cylinders) turbo charged diesel engine equipped with VGT and EGR, was collected in test cell. The data was then used to build and validate different static models, which were later applied to dynamic modelling and validation.

Target group

This thesis is aimed for engineers and students, with basic knowledge in the area of vehicular systems.

Chapter 2

Measurements

To build and validate a model, engine data is required. Data is collected in an engine test cell on a Scania (12 liter, 6 cylinders) turbo charged diesel engine, equipped with VGT and EGR. The test engine is equipped with a lot of extra sensors, compared to a normal engine, to simplify model building and validation. An explanatory sketch of the test engine, and where different variables are measured, can be seen in Figure 2.1.

The mass flow through the inlet manifold (W_{im}) is measured before the intercooler (IC). During static operation this does not cause any problems as there is no change of mass in the intercooler. During transients, the measured mass flow through the inlet manifold ($W_{im,meas}$) and W_{im} are not the same due to filling or emptying of the intercooler. When looking at transients, small or no difference in mass flow was found when trying to compensate for the intercooler dynamics, compared with when no compensation was made. Therefore $W_{im,meas}$ is assumed accurate.

Inlet manifold pressure (p_{im}) and temperature (T_{im}) are measured after the intercooler. Exhaust manifold pressure (p_{em}) and temperature (T_{em}) are measured right before the turbine. Engine torque (M_e) and engine speed (n_e) are also measured and the position of the corresponding sensors, can be seen in Figure 2.1.

All the measurements are made at constant engine speed. Load and air mass flow are altered by changing e.g. injected fuel amount (δ), start of injection (α) and the geometry of the turbine. During static measurements, all the variables are measured for 75 seconds and then a mean value is stored. During continuous measurements, all the variables are stored every tenth of a second.

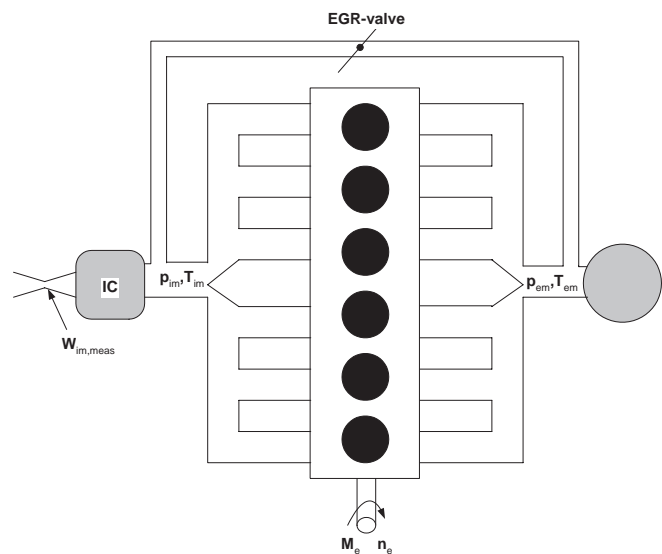


Figure 2.1: Explanatory sketch of the test engine and where important variables are measured.

Chapter 3

Modelling

In this chapter two approaches, for building a model for T_{em} , are presented. The first one is based on an energy balance of the combustion chamber, Section 3.1, and the other is based on ideal cycle calculations, Section 3.2. The latter includes calculations on the Otto and Seliger cycle of which the Seliger cycle should give the better approximation to a diesel engine [8]. In Section 3.3 a procedure, of how to apply these models to dynamic measurements, is proposed.

3.1 Energy Balance Model

Rewriting the first law of thermodynamics, an energy balance of the combustion chamber can be derived [3, 7],

$$W_{im}c_p(T_{im} - T_{em}) + \dot{Q}_{fuel} - \dot{Q}_{tp} - \dot{Q}_{ht} = 0, \quad (3.1)$$

where

$$W_{im}c_p(T_{im} - T_{em})$$

is the change of energy due to increase of gas temperature from inlet to outlet manifold. The change of energy due to mass flow of fuel (W_{fuel}) to the engine,

$$\dot{Q}_{fuel} = W_{fuel}q_{HV} \propto \delta n_e q_{HV},$$

the power produced by the engine,

$$\dot{Q}_{tp} \propto M_e n_e$$

and \dot{Q}_{ht} is the heat transfer to the combustion chamber walls. Solving (3.1) for T_{em} gives

$$T_{em} = T_{im} + \frac{\dot{Q}_{fuel} - \dot{Q}_{tp} - \dot{Q}_{ht}}{W_{im}c_p}, \quad (3.2)$$

which will be referred to as the energy balance model. An estimation of \dot{Q}_{ht} ,

$$f_{ht}^1 = f_{ht}^1(\delta, W_{im}, \alpha, n_e), \quad (3.3)$$

is derived from data.

The difference in cooling water temperature before and after the engine, ΔT_{water} , can also be used when estimating \dot{Q}_{ht} . The heat released in the combustion chamber heats the cylinder walls which are cooled by the cooling water. The mass flow of cooling water is kept constant during measurements. Knowing this, the heat transfer to the cooling water is proportional to ΔT_{water} and the mass flow is left out of the formula,

$$f_{ht}^2 = f_{ht}^2(\delta, W_{im}, \alpha, n_e, \Delta T_{water}), \quad (3.4)$$

which should estimate \dot{Q}_{ht} better than f_{ht}^1 , and therefore give smaller errors.

One problem with the energy balance model is that M_e is not measured in series production trucks, and the engine torque is not easy to model with good accuracy. Another problem is that the combustion process is very complex and f_{ht}^i are only close to correct when building and validating the model at similar engine conditions.

3.2 Ideal Cycle Models

In this section an engine cycle (intake, compression, combustion, expansion and exhaust) is modelled with two different ideal cycles, the Otto (constant volume) cycle and the Seliger (limited pressure) cycle. The formulas presented here are results of calculations on ideal cycle models. For assumptions and derivation of formulas, see Appendix A.

Indices 1 (after intake), 2 (before combustion) and 3 (after combustion) may appear on pressures, temperatures and specific volume (v), which refer to the value of the variables at that specific state.

3.2.1 Otto Cycle

From Otto cycle calculations, the exhaust gas temperature,

$$T_{em} = \eta_{oc} T_1 \left(\frac{p_{em}}{p_{im}} \right)^{1-1/\gamma} \left(1 + \frac{q_{in}}{c_v T_1 \left(\frac{v_1}{v_2} \right)^{\gamma-1}} \right)^{1/\gamma}, \quad (3.5)$$

is given, where η_{oc} is a compensation factor for non ideal cycles. Further, the specific energy content of the charge per unit mass,

$$q_{in} = \frac{W_{fuel} q_{HV}}{W_{im} + W_{fuel}} (1 - x_r), \quad (3.6)$$

the residual gas fraction,

$$x_r = \frac{v_2}{v_1} \left(\frac{p_{em}}{p_{im}} \right)^{1/\gamma} \left(1 + \frac{q_{in}}{c_v T_1 \left(\frac{v_1}{v_2} \right)^{\gamma-1}} \right)^{-1/\gamma} \quad (3.7)$$

and

$$T_1 = x_r T_{em} + (1 - x_r) T_{im}. \quad (3.8)$$

Solving (3.5) for η_{oc} gives

$$\eta_{oc} = \left(\frac{T_{em}}{T_1} \right) \left(\frac{p_{em}}{p_{im}} \right)^{1/\gamma-1} \left(1 + \frac{q_{in}}{c_v T_1 \left(\frac{v_1}{v_2} \right)^{\gamma-1}} \right)^{-1/\gamma}. \quad (3.9)$$

The exhaust gas temperature can not be solved analytically from the full model, (3.5) to (3.9), as the equations depend on each other. A numeric solver is used for (3.5) to (3.9), when building the model and for (3.5) to (3.8), when validating it. When validating the model η_{oc} is not calculated from (3.9). Instead

$$\eta_{oc} = \eta_{oc}(\delta, W_{im}, \alpha, n_e) \quad (3.10)$$

is calculated from engine data.

3.2.2 Seliger Cycle

From Seliger cycle calculations, the exhaust gas temperature,

$$T_{em} = \eta_{sc} \left(\frac{p_{em}}{p_{im}} \right)^{1-1/\gamma} \left(\frac{v_2}{v_1} \right)^{\gamma-1} \left(1 + \frac{q_{in}}{c_v T_1 \left(\frac{v_1}{v_2} \right)^{\gamma-1} x_{cv}} \right)^{1/\gamma-1} * \\ * \left(q_{in} \left(\frac{1 - x_{cv}}{c_p} + \frac{x_{cv}}{c_v} \right) + T_1 \left(\frac{v_1}{v_2} \right)^{\gamma-1} \right), \quad (3.11)$$

is given, where η_{sc} is a compensation factor for non ideal cycles and x_{cv} the ratio of fuel consumed during constant volume combustion (when $x_{cv} = 1$, the Seliger cycle is the same as the Otto cycle). The rest of the fuel is used during constant pressure combustion. Further, T_1 and q_{in} as in (3.8) and (3.6) where,

$$x_r = \frac{v_2}{v_1} \frac{v_2}{v_3} \left(\frac{p_{em}}{p_{im}} \right)^{1/\gamma} \left(1 + \frac{q_{in}}{c_v T_1 \left(\frac{v_1}{v_2} \right)^{\gamma-1} x_{cv}} \right)^{-1/\gamma}, \quad (3.12)$$

$$v_3 = v_2 \left(1 + \frac{q_{in}}{c_p \left(\frac{q_{in}}{c_v} x_{cv} + T_1 \left(\frac{v_1}{v_2} \right)^{\gamma-1} \right)} (1 - x_{cv}) \right) \quad (3.13)$$

and η_{sc} can be solved from (3.11). As in Section 3.2.1 a numeric solver is used and x_{cv} has to be fixed before starting. The ratio x_{cv} is highly dependant of start of combustion (SOC), which is dependant on e.g. α and W_{im} . No model for x_{cv} is presented but is instead assumed constant.

When validating the model η_{sc} is not calculated from (3.11). Instead

$$\eta_{sc} = \eta_{sc}(\delta, W_{im}, \alpha, n_e)$$

is calculated from engine data.

3.2.3 Summary

The Otto cycle model is a special case of the Seliger cycle model. Yet it is interesting to validate both models to see whether x_{cv} makes a difference. With access to T_{im} , W_{im} , W_{fuel} , p_{im} and p_{em} , the models estimate the exhaust gas temperature. Both models use a compensation factor, η_{oc} and η_{sc} , that can either be fit to measured data or set to 1.

3.3 Dynamic Modelling

None of the models in this chapter has any state variables. Heating and cooling effects of the engine is not modelled so no good results during transients can be expected. There are low-pass sensor dynamics in the temperature sensors. To make the modelled exhaust gas temperature ($T_{em,mod}$) comparable with the measured ($T_{em,meas}$), the former is filtered with a first order low-pass filter. The time constant for this filter is set constant (4 s) and might also capture some heating and cooling effects of the engine.

Chapter 4

Validation

In this chapter the models presented in Chapter 3 are validated. The geometry of the VGT, α and δ are manipulated to give a wide range of T_{em} (550–950 K) during static validation. For dynamic validation load transients are used. To get the most accurate measurement of W_{im} , the EGR valve is kept closed. Engine speed is kept constant. This is a major simplification, compared to letting the engine speed change, but the validations are still interesting. Since having found a model that is good at one engine speed, it is easy to build such a model for other engine speeds, and interpolate between the models. The reason why only one engine speed is validated is that collection of data is time consuming and expensive.

As all of the models in Chapter 3 are in some way based on engine data, there is a difference between building and validating the model at different and similar engine conditions. Building and validating models at similar engine conditions should give a smaller error. Doing the same at different engine conditions should give an indication of the physical correctness of the model. There is therefore more than one validation for every model.

Results are presented with, mean and maximum

$$\text{Absolute error} = |T_{em,meas} - T_{em,mod}|$$

and

$$\text{Relative error} = \frac{|T_{em,meas} - T_{em,mod}|}{T_{em,meas}},$$

for all validations.

Table 4.1: Results of the validations in Section 4.1, for the energy balance model, when comparing measured and modelled T_{em} .

Validation	Abs. error (K)		Rel. error (%)	
	mean	max	mean	max
1	27.6	71.3	3.0	7.7
2	15.9	47.6	2.3	8.7
3	14.8	46.2	1.6	4.8
4	12.0	24.4	1.6	3.2

Table 4.2: Results of the validations in Section 4.2.1, for the Otto cycle model, when comparing measured and modelled T_{em} .

Validation	Abs. error (K)		Rel. error (%)	
	mean	max	mean	max
1	40.5	107.8	4.7	11.5
2	27.5	50.0	3.6	5.3
3	7.0	17.5	0.8	2.1
4	5.8	13.7	0.8	1.9

4.1 Energy Balance Model Validation

In this section the model presented in (3.2), with \dot{Q}_{ht} estimated with f_{ht}^i , is validated.

Validation 1: In (3.3), f_{ht}^1 is fitted to engine conditions different from the validating data.

Validation 2: In (3.3), f_{ht}^1 is fitted to engine conditions similar to the validating data.

Validation 3: In (3.4), f_{ht}^2 is fitted to engine conditions different from the validating data. The difference in cooling water temperature before and after the engine, ΔT_{water} , is used.

Validation 4: In (3.4), f_{ht}^2 is fitted to engine conditions similar to the validating data. The difference in cooling water temperature before and after the engine, ΔT_{water} , is used.

The results of the four different validations with different f_{ht}^i (estimations of \dot{Q}_{ht}) are presented in Table 4.1. As predicted in Section 3.1 the tabel show (compare relative errors for validation 2 with 4 or 1 with 3) that better results are achieved when ΔT_{water} is used in the estimation of \dot{Q}_{ht} .

4.2 Ideal Cycle Model Validation

In this section the ideal cycle models from Section 3.2, are validated. Some observations, for the validations, are found in Section 4.2.3.

4.2.1 Otto Cycle

In this section the Otto cycle model presented in (3.5) to (3.9) is validated.

Validation 1: The compensation factor, η_{oc} , is kept constant at 1 so there is no fit to measured data. The α recommended by S6 (Scania's engine control system) is not used but α is varied manually at different loads. The VGT is constant at same load.

Validation 2: The compensation factor, η_{oc} , is kept constant at 1 so there is no fit to measured data. The VGT is varied at different loads and α is chosen by S6.

Validation 3: The compensation factor, η_{oc} , is fitted to engine conditions different from the validating data.

Validation 4: The compensation factor, η_{oc} , is fitted to engine conditions similar to the validating data.

The results of the four different validations are presented in Table 4.2.

4.2.2 Seliger Cycle

In this section the model presented in Section 3.2.2 is validated.

Validation 1: The compensation factor, η_{sc} , is kept constant at 1 so there is no fit to measured data. The α recommended by S6 is not used but α is varied manually at different loads. The VGT is constant at same load.

Validation 2: The compensation factor, η_{sc} , is kept constant at 1 so there is no fit to measured data. The VGT is varied at different loads and α is chosen by S6.

Validation 3: The compensation factor, η_{sc} , is fitted to engine conditions different from the validating data.

Validation 4: The compensation factor, η_{sc} , is fitted to engine conditions similar to the validating data.

The results of the four different validations are presented in Table 4.3. Measured and modelled T_{em} , for two of the validations, are presented in figures referred to from Table 4.3.

Table 4.3: Results of the validations in Section 4.2.2, for the Seliger cycle model, when comparing measured and modelled T_{em} .

Validation	Figure	Abs. error (K)		Rel. error (%)	
		mean	max	mean	max
1	4.1	34.2	87.9	4.2	9.4
2	4.2	16.1	26.9	2.3	4.9
3	—	6.5	16.2	0.8	2.0
4	—	5.5	12.8	0.8	1.7

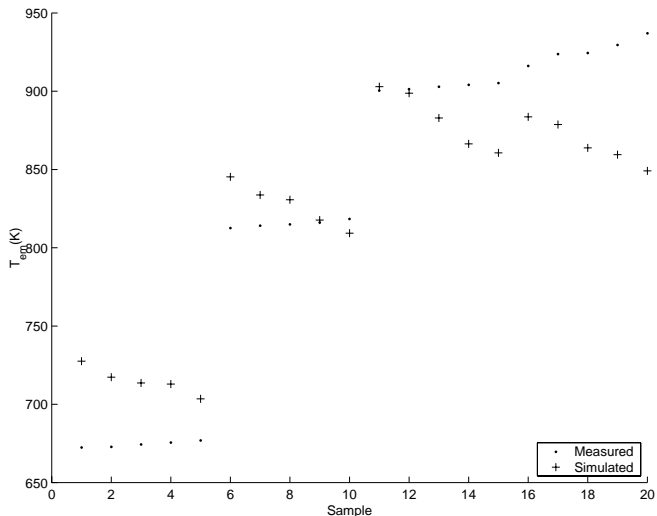


Figure 4.1: Measured and modelled T_{em} (for the Seliger cycle model) for changes in α at different loads. No fit to data.

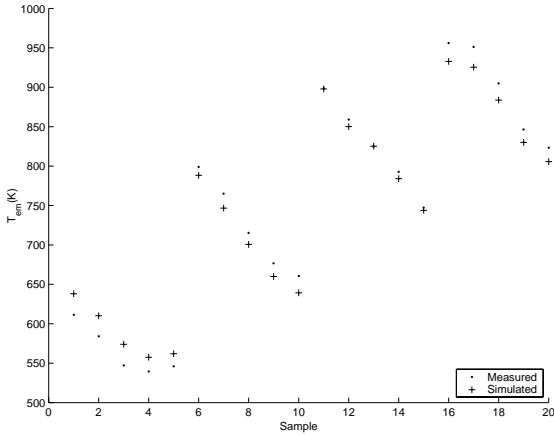


Figure 4.2: Measured and modelled T_{em} (for the Seliger cycle model) for changes of the VGT at different loads. No fit to data.

4.2.3 Validation Observations for the Ideal Cycles

When η (both η_{oc} and η_{sc}) is kept at 1 (no fit to data), there is a big difference between the results for validation 1 and 2 (compare relative errors for validation 1 and 2 in e.g. Table 4.3). To show this, not only in numbers, some samples in the validation figures for the Seliger cycle model can be discussed.

In Figure 4.1 samples 6–10, $T_{em,meas}$ increases but $T_{em,mod}$ decreases, which means that the Seliger cycle model does not capture changes in α . Comparing with the same samples in Figure 4.2, it is obvious that changes in the VGT is captured much better than changes in α .

The α chosen by S6 is set to give a combustion that can be seen as normal for the engine. When α is altered without any thought of this (validation 1), the combustion is less ideal and the ideal cycle models show poorer results, than when α is chosen by S6 (validation 2).

The relative errors for validations 3 and 4 are almost the same. When fitting η to engine data, it is therefore not crucial to have engine data similar to the validating data. This is good as it takes a lot of work to collect data from every engine setting, when building the model.

The relative errors for the Seliger cycle model (Table 4.3) are smaller or equal than the ones for the Otto cycle model (Table 4.2). This indicates that x_{cv} makes a difference to the Seliger cycle validation results (remember that the Otto cycle is a special case of the Seliger cycle with $x_{cv} = 1$). The Seliger cycle's x_{cv} is highly dependant on α , but is in this work set constant. A better model for x_{cv} should capture changes in α better, and give better results for validation 1.

Table 4.4: Results for all three models for load transient: 50-75-50%, when comparing measured and modelled T_{em} .

Model	Figure	Abs. error (K)		Rel. error (%)	
		mean	max	mean	max
Energy balance	4.3 (a)	9.1	35.8	1.1	4.2
Otto	4.3 (b)	3.5	10.1	0.4	1.2
Seliger	4.3 (c)	3.6	10.2	0.4	1.2

4.3 Dynamic Validation

All transients are load transients (steps up or down in δ) at engine speed 1434 rpm. If the caption says “Load transient: 50-100-75%”, it means that δ begins at 50% of its maximum, increased to 100% and at last lowered to 75%. When the models are fit to measured data, static measurements with conditions similar to the ones during the transients are used.

When there is no filtering of $T_{em,mod}$, the modelled temperature is much higher than $T_{em,meas}$, right after an increase in load (compare Figures 4.3 (c) and (d)), which partly can be explained by sensor dynamics. Another explanation could be that $W_{im,meas}$ and the real W_{im} differ from each other, due to filling and emptying of the intercooler, during transients. If $W_{im,meas} < W_{im}$ right after an increase of load, all the models will calculate a higher $T_{em,mod}$ than if $W_{im,meas} = W_{im}$.

As pointed out before (Section 3.3) none of the models has any dynamics except for the low-pass filtering of $T_{em,mod}$. Knowing this a comparison between the three models is made only for one load transient and the best model is then further validated. A comparison (Figure 4.3 (a), (b) and (c) and Table 4.4) between the different models for a load transient: 50-75-50% is made. The relative errors in Table 4.4 are much smaller for the ideal cycle models than for the energy balance model. During transients ΔT_{water} was not measured so the energy balance model could have given better results. As the Seliger cycle model give better results than both the energy balance and the Otto cycle model, during static validation (compare relative errors for e.g. validation 4 in Table 4.1, 4.2 and 4.3), the Seliger cycle model is the one further validated.

The results of a comparison between the Seliger model with and without estimated η_{sc} , for load transients can be seen in Figure 4.4 and Table 4.5. The difference in error (compare relative errors for same load in Table 4.5) does not seem to come from the dynamic behavior but instead from when $T_{em,meas}$ is close to stable in between the steps in δ (compare Figure 4.4 (a) with (b) or (c) with (d)).

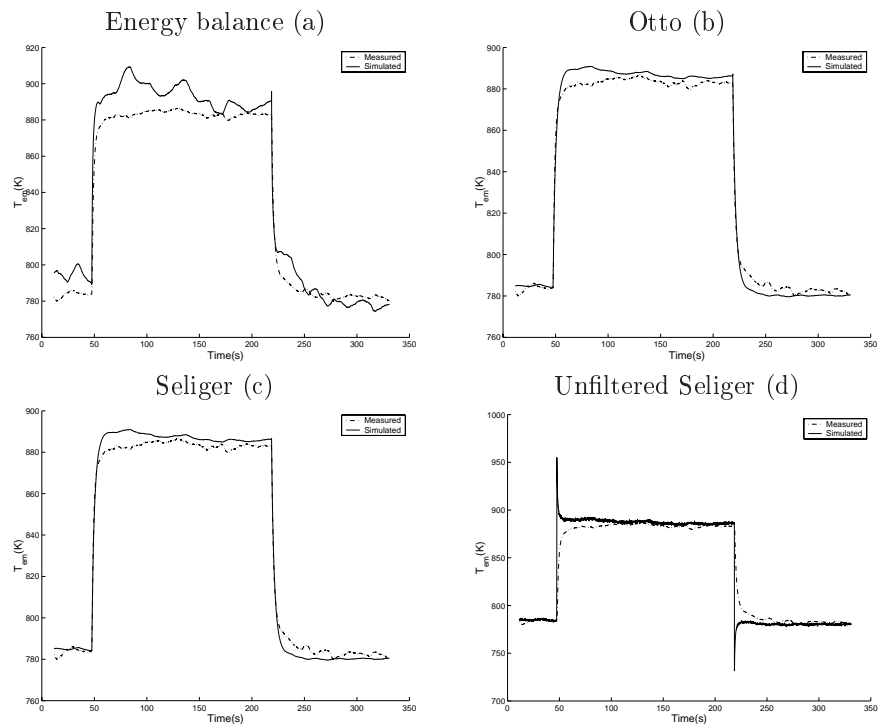


Figure 4.3: Measured and modelled T_{em} for comparison between Energy balance (a), Otto (b) and Seliger (c) model for load transient: 50-75-50%. Also comparison between filtered (c) and unfiltered (d) Seliger model for same transient.

Table 4.5: Results for the Seliger cycle model with and without estimated η_{sc} , for load transients, when comparing measured and modelled T_{em} . Upper row for each load is for when η_{sc} is estimated and lower is for when $\eta_{sc} = 1$ (no fit to data).

Load	Figure	Abs. error (K)		Rel. error (%)	
		mean	max	mean	max
25-50-25%	4.4 (a)	7.0	20.7	1.0	3.1
25-50-25%	4.4 (b)	19.1	38.8	2.6	5.0
50-75-50%	4.4 (c)	3.6	10.2	0.4	1.2
50-75-50%	4.4 (d)	13.2	22.4	1.6	2.8

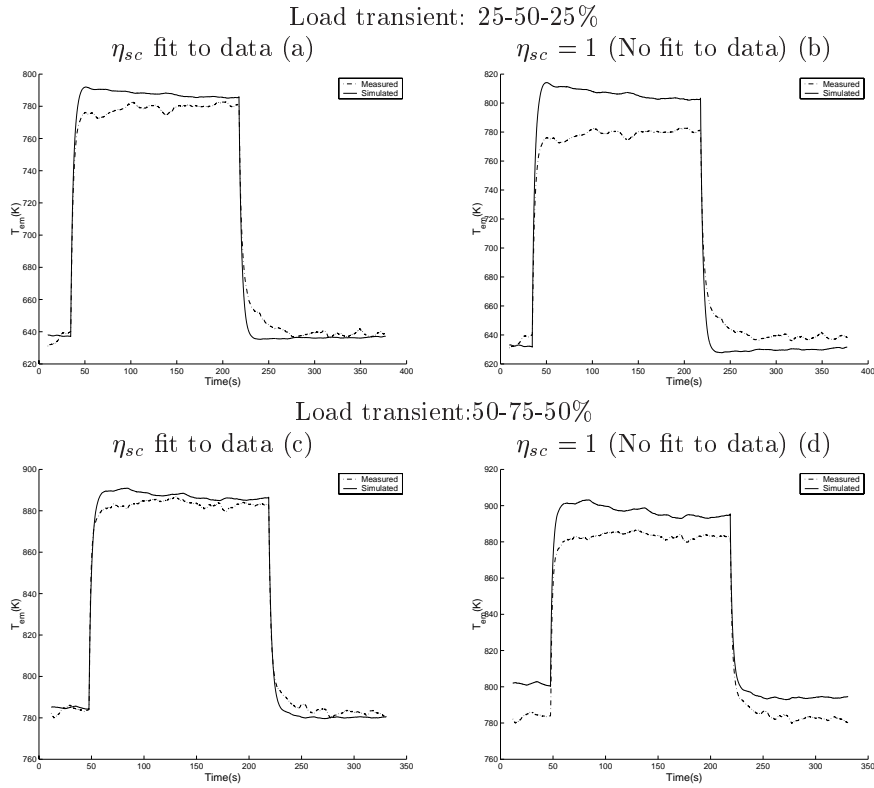


Figure 4.4: Measured and modelled T_{em} , for load transients, for comparison between Seliger models with ((a) and (c)) and without ((b) and (d)) estimated η_{sc} .

4.4 Summary

The Seliger cycle model show better results than the other two models during static validation. As the dynamic behaviour is the same for all models, the model with the best static results should also show the best results during transients. Therefore the Seliger cycle model is suggested as the model of choice.

During static validation the suggested model show the following results. The Seliger cycle model fit to engine data show a maximum relative error of 2% (Table 4.3 validations 3 and 4). With no fit to engine data and α chosen by S6, the same model show a maximum relative error of 5% (Table 4.3 validation 2). When α is not chosen by S6, but changed manually, relative errors up to 10% (Table 4.3 validation 1) can occur when there is no fit to data. As the engine runs with α chosen by S6 this is not a problem at the engine speed chosen for validation.

Chapter 5

Conclusions and Future Work

This chapter summarizes the conclusions drawn in this thesis and give some suggestions for future work on the models.

5.1 Conclusions

An extension of the ideal Seliger cycle is suggested as the model of choice. Some results and observations for the Seliger cycle are given below. For further results for the Seliger model and results for the other models, please refer to Chapter 4.

Static Validation

An extension of the ideal Seliger cycle proved to give the best results for static validation. With access to T_{im} , W_{im} , W_{fuel} , p_{im} and p_{em} , the Seliger cycle model estimates the exhaust gas temperature. When T_{em} is varied (by changing the VGT, α and δ) between 550 K and 950 K at constant engine speed, static validations with model fit to engine data show a maximum relative error of 2% (Table 4.3 validations 3 and 4). With no fit to engine data and α chosen by S6 (Scania's engine control system), the same model show a maximum relative error of 5% (Table 4.3 validation 2). When α is not chosen by S6, but changed manually, relative errors up to 10% (Table 4.3 validation 1) can occur when there is no fit to data. As the engine runs with α chosen by S6 this is not a problem at the engine speed chosen for validation.

Dynamic Validation

With the simple low-pass filtering of $T_{em,mod}$ all the tested models have about the same dynamic behaviour during load transients. The conclusion to be drawn from this is to use the model with the best static validation results which is the Seliger cycle model.

5.2 Future Work

This section suggests topics for future work with the different models.

Cylinder Wall Temperature

None of the models take heating/cooling effects of the engine into account during transients. A dynamic model for the cylinder wall temperature would here be useful, but not easy to make. Such a model could, besides giving better dynamic behaviour, also help estimating the heat transfer better for the energy balance model. Inspiration to such a model can be found in [6].

The Ratio of Fuel Consumed during Constant Volume

The ratio of fuel consumed during constant volume (x_{cv}), in the Seliger cycle model, is in this work set constant. A model for x_{cv} that changes with e.g. SOC should give better results overall, and maybe give an explanation to the bad results when α is not chosen by S6 (for when there is no fit to data). Further studies of measured engine cycles should be of help to model x_{cv} .

Engine Torque

Ideal cycle calculations can, theoretically, quite easily give the engine torque. When doing this for the Seliger cycle model with constant x_{cv} there was no good agreement between measured and calculated engine torque. With a better model for x_{cv} this should be a good approach in estimating the engine torque.

References

- [1] Håkan Bengtsson. Modelling of volumetric efficiency on a diesel engine with variable geometry turbine. Master's thesis LiTH-ISY-EX-3379, Department of Electrical Engineering, Linköpings Universitet, Linköping, Sweden, 2002.
- [2] Sven Öberg. Identification and improvement of an – automotive diesel engine model purposed – for model based diagnosis. Master's thesis LiTH-ISY-EX-3161, Department of Electrical Engineering, Linköpings Universitet, Linköping, Sweden, 2001.
- [3] Sixten Berglund. Comparison between measured and simulated transients of a turbocharged diesel engine. *SAE Paper No. 942323*, 1994.
- [4] Jonas Biteus. Mvem of dc12 scania engine internal scania report. Technical report, Department of Electrical Engineering, Linköpings universitet, Linköping, Sweden, 2002.
- [5] David Elfvik. Modelling of a diesel engine with vgt – for control design simulations. Master's thesis, KTH, Stockholm, Sweden, 2002.
- [6] Lars Eriksson. Mean value models for exhaust system temperatures. *SAE Paper No. 2002-01-0374*, 2002.
- [7] Jonas Fredriksson. *Nonlinear Control of Turbocharged Diesel Engines, An integrated powertrain control perspective*. Lic thesis, Department of Signals and Systems, Chalmers University of Technology, Göteborg, Sweden, 1999.
- [8] John B. Heywood. *Internal Combustion Engine Fundamentals*. McGraw-Hill, Singapore, 1987.
- [9] Martin Muller, Elbert Hendricks, and Spencer Sorensen. Mean value modelling of turbocharged spark ignition engines. *SAE Paper No. 980784*, 1998.

- [10] Lars Nielsen and Lars Eriksson. Course material, vehicular systems. Department of Electrical Engineering, Linköpings universitet, Linköping, Sweden, 2001.
- [11] Mattias Nyberg and Erik Frisk. Diagnosis and supervision of technical processes. Department of Electrical Engineering, Linköpings universitet, Linköping, Sweden, 2001.

Notation

Table 5.1: Symbols used in the report.

Symbol	Value	Description	Unit
α	Act	Start of injection	degrees
γ	c_p/c_v	—	—
ΔT_{water}	Var	Difference in cooling water temperature before and after the engine	K
δ	Act	Amount of injected fuel	kg/stroke
η	-	Compensation factor for non ideal cycles	—
c_p	Con	Specific heat capacity at constant pressure	J/(kg · K)
c_v	Con	Specific heat capacity at constant volume	J/(kg · K)
M_e	Var	Engine torque	Nm
n_e	Var	Engine speed	rpm
n_r	2	Revolutions per cycle	—
N_{cyl}	6	Number of cylinders	—
p	Var	Pressure	Pa
q_{HV}	Con	Heating value	J/kg
q_{in}	Var	Specific energy content of the charge per unit mass	J/kg
Q	Var	Energy	J
\dot{Q}	Var	Power	W
T	Var	Temperature	K
v	Var	Specific volume	m^3/kg
V	Var	Volume	m^3
W	Var	Mass-flow	kg/s
x_{cv}	Con	Ratio of fuel consumed during constant volume	—
x_r	Var	Residual gas fraction	—

Table 5.2: Abbreviations used in this report.

Abbreviation	Explanation
Con	Constant
Var	Variable
Act	Actuator
EGR	Exhaust Gas Recirculation
SOC	Start Of Combustion
rpm	Revolutions Per Minute
VGT	Variable Geometry Turbine
IC	Intercooler
S6	Scania's engine control system
OBD	On-Board Diagnostics

Table 5.3: Indices used in this report.

Index	Explanation
em	Exhaust manifold
im	Inlet manifold
oc	Otto cycle
sc	Seliger cycle
tp	Torque production
ht	Heat transfer
1–8	Different states in ideal cycle
meas	Measured
mod	Modelled

Appendix A

Ideal Cycle Calculations

A four stroke diesel engine goes through four different strokes during an engine cycle: intake, compression, combustion and exhaust stroke. This cycle can be modelled with different ideal cycles and will in this appendix be exemplified by the ideal Otto (constant volume cycle) and Seliger cycle (limited pressure cycle). Similar calculations to the ones made in this appendix can be seen in e.g. [8, 10]. They will here be presented for each state of the ideal cycle, but not always explained. The general assumptions in the following sections are that the gases are ideal and that c_v and c_p are constants. Just as a comparison with the ideal cycle models presented in this chapter, a measured engine cycle, Figure A.1, is included. Consult the Notation when needed.

A.1 Otto Cycle

The indices in the equations below refer to the different states in Figure A.2.

Compression (1–2)

$$p_2 = p_1 \left(\frac{v_1}{v_2} \right)^\gamma \quad (\text{A.1})$$

$$T_2 = T_1 \left(\frac{v_1}{v_2} \right)^{\gamma-1} \quad (\text{A.2})$$

Combustion (2–3)

$$q_{in} = \frac{W_{fuel} q_{HV}}{W_{im} + W_{fuel}} (1 - x_r)$$

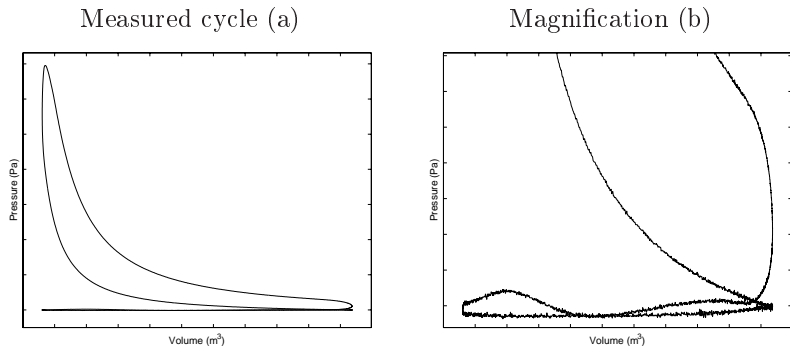


Figure A.1: p-V diagram for a measured cycle (a) with a magnification of the intake and exhaust stroke (b).

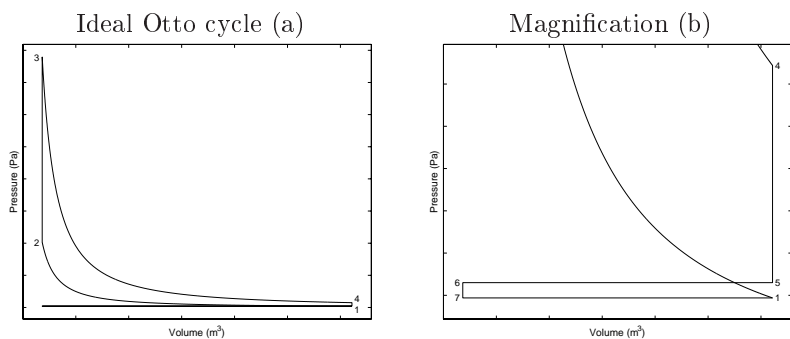


Figure A.2: p-V diagram for an ideal Otto cycle (a) with a magnification of the intake and exhaust stroke (b). As $p_{em} > p_{im}$, p_5 and p_6 are higher than p_1 and p_7 respectively.

$$p_3 = p_2 \left(1 + \frac{q_{in}}{c_v T_2} \right) \quad (\text{A.3})$$

$$T_3 = T_2 + \frac{q_{in}}{c_v} \quad (\text{A.4})$$

Expansion (3–4)

$$p_4 = p_3 \left(\frac{v_3}{v_4} \right)^\gamma \quad (\text{A.5})$$

$$T_4 = T_3 \left(\frac{v_3}{v_4} \right)^{\gamma-1} \quad (\text{A.6})$$

Blowdown (4–5)

$$p_5 = p_{em}$$

$$T_5 = T_{em} = T_4 \left(\frac{p_{em}}{p_4} \right)^{1-1/\gamma} \quad (\text{A.7})$$

Exhaust (5–6)

$$p_6 = p_{em}$$

$$T_6 = T_{em}$$

At state 6 there is some residual gas trapped in the cylinder. This mass, m_r , divided by the total mass of the gas in the cylinder at e.g. state 4, m_t is called the residual gas fraction x_r . Using the Ideal gas law at state 4 and 6 gives

$$x_r = \frac{m_r}{m_t} = \frac{V_6}{V_4} \frac{p_{em}}{p_4} \frac{T_4}{T_e} = \frac{V_6}{V_4} \left(\frac{p_e}{p_4} \right)^{1/\gamma}. \quad (\text{A.8})$$

Intake valve opening (6–7)

$$p_7 = p_{im}$$

$$T_7 = T_{em}$$

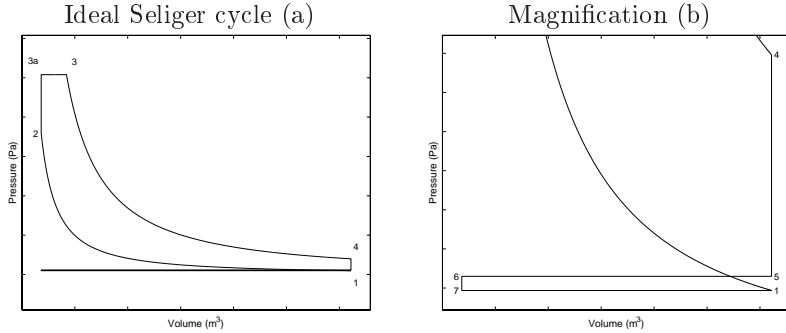


Figure A.3: p-V diagram for an ideal Seliger cycle (a) with a magnification of the intake and exhaust stroke (b). As $p_{em} > p_{im}$, p_5 and p_6 are higher than p_1 and p_7 respectively.

Intake (7–1)

$$p_1 = p_{im} \quad (\text{A.9})$$

$$T_1 = x_r T_{em} + (1 - x_r) T_{im} \quad (\text{A.10})$$

Using (A.7), assuming that $v_4 = v_1$ and $v_3 = v_2$, with (A.1), (A.2), (A.3), (A.4), (A.5), (A.6) and (A.9) gives

$$T_{em} = T_1 \left(\frac{p_{em}}{p_{im}} \right)^{1-1/\gamma} \left(1 + \frac{q_{in}}{c_v T_1 \left(\frac{v_1}{v_2} \right)^{\gamma-1}} \right)^{1/\gamma}. \quad (\text{A.11})$$

Using (A.8), assuming that $v_4 = v_1$, $V_6 = V_2$ and $v_3 = v_2$, with (A.1), (A.2), (A.3) and (A.5) gives

$$x_r = \frac{v_2}{v_1} \left(\frac{p_{em}}{p_{im}} \right)^{1/\gamma} \left(1 + \frac{q_{in}}{c_v T_1 \left(\frac{v_1}{v_2} \right)^{\gamma-1}} \right)^{-1/\gamma}. \quad (\text{A.12})$$

(A.10), (A.11) and (A.12) are the same as (3.8), (3.5) and (3.7) except that (3.5) has a factor η_{oc} to compensate for non ideal cycles.

A.2 Seliger Cycle

The indices in the equations below refer to the different states in Figure A.3.

Compression (1–2)

$$p_2 = p_1 \left(\frac{v_1}{v_2} \right)^\gamma \quad (\text{A.13})$$

$$T_2 = T_1 \left(\frac{v_1}{v_2} \right)^{\gamma-1} \quad (\text{A.14})$$

Constant volume combustion (2–3a)

$$q_{in} = \frac{W_{fuel} q_{HV}}{W_{im} + W_{fuel}} (1 - x_r) \quad (\text{A.15})$$

$$p_{3a} = p_2 \left(1 + \frac{q_{in}}{c_v T_2} x_{cv} \right) \quad (\text{A.15})$$

$$T_{3a} = T_2 + \frac{q_{in}}{c_v} x_{cv} \quad (\text{A.16})$$

Where x_{cv} is the ratio of fuel that is consumed during constant volume combustion. The rest of the fuel is assumed to go to constant pressure combustion.

Constant pressure combustion (3a–3)

$$p_3 = p_{3a} \quad (\text{A.17})$$

$$T_3 = T_{3a} \frac{v_3}{v_{3a}} \quad (\text{A.18})$$

$$T_3 = T_{3a} + \frac{q_{in}}{c_p} (1 - x_{cv}) \quad (\text{A.19})$$

Expansion (3–4)

$$p_4 = p_3 \left(\frac{v_3}{v_4} \right)^\gamma \quad (\text{A.20})$$

$$T_4 = T_3 \left(\frac{v_3}{v_4} \right)^{\gamma-1} \quad (\text{A.21})$$

Blowdown (4–5)

$$p_5 = p_{em}$$

$$T_5 = T_{em} = T_4 \left(\frac{p_{em}}{p_4} \right)^{1-1/\gamma} \quad (\text{A.22})$$

Exhaust (5–6)

$$p_6 = p_{em}$$

$$T_6 = T_{em}$$

Intake valve opening (6–7)

$$p_7 = p_{im}$$

$$T_7 = T_{em}$$

Intake (7–1)

$$p_1 = p_{im} \quad (\text{A.23})$$

$$T_1 = x_r T_{em} + (1 - x_r) T_{im} \quad (\text{A.24})$$

Using (A.22), assuming that $v_4 = v_1$ and $v_{3a} = v_2$, with (A.13), (A.14), (A.15), (A.16), (A.17), (A.19), (A.20), (A.21) and (A.23) gives

$$\begin{aligned} T_{em} &= \left(\frac{p_{em}}{p_{im}} \right)^{1-1/\gamma} \left(\frac{v_2}{v_1} \right)^{\gamma-1} \left(1 + \frac{q_{in}}{c_v T_1 \left(\frac{v_1}{v_2} \right)^{\gamma-1}} x_{cv} \right)^{1/\gamma-1} * \\ &* \left(q_{in} \left(\frac{1 - x_{cv}}{c_p} + \frac{x_{cv}}{c_v} \right) + T_1 \left(\frac{v_1}{v_2} \right)^{\gamma-1} \right). \end{aligned} \quad (\text{A.25})$$

Using (A.18), assuming $v_{3a} = v_2$, v_3 , with (A.14), (A.16) and (A.19) gives

$$v_3 = v_2 \left(1 + \frac{q_{in}}{c_p \left(\frac{q_{in}}{c_v} x_{cv} + T_1 \left(\frac{v_1}{v_2} \right)^{\gamma-1} \right)} (1 - x_{cv}) \right). \quad (\text{A.26})$$

Using (A.8), assuming that $v_4 = v_1$ and $V_6 = V_2$, with (A.13), (A.14), (A.17) and (A.20) gives

$$x_r = \frac{v_2}{v_1} \frac{v_2}{v_3} \left(\frac{p_{em}}{p_{im}} \right)^{1/\gamma} \left(1 + \frac{q_{in}}{c_v T_1 \left(\frac{v_1}{v_2} \right)^{\gamma-1}} x_{cv} \right)^{-1/\gamma}. \quad (\text{A.27})$$

With simple calculations it is obvious that the Otto cycle is a special case of the Seliger cycle with $x_{cv} = 1$.

(A.24), (A.25) and (A.27) are the same as (3.8), (3.11) and (3.12) except that (3.11) has a factor η_{sc} to compensate for non ideal cycles.